

OCT 22 1945

# NATIONAL ADVISORY COMMITTEE FOR AERONAUTICS

TECHNICAL NOTE

No. 992

EFFECT OF FATIGUE-STRESSING SHORT OF FAILURE  
ON SOME TYPICAL AIRCRAFT METALS

By J. A. Bennett  
National Bureau of Standards



Washington  
October 1945

NACA LIBRARY  
LANGLEY MEMORIAL AERONAUTICAL  
LABORATORY  
Langley Field, Va.

NATIONAL ADVISORY COMMITTEE FOR AERONAUTICS

TECHNICAL NOTE NO. 992

EFFECT OF FATIGUE-STRESSING SHORT OF FAILURE

ON SOME TYPICAL AIRCRAFT METALS

By J. A. Bennett

SUMMARY

A number of tests were made to determine the effect of service stresses on the impact resistance, the X-ray diffraction patterns, and the microstructure of 25S aluminum alloy. The average impact resistance was found to be unimpaired even in material cut from specimens previously broken by repeated stress. The X-ray diffraction patterns showed no structural change resulting from the fatigue-stressing of the alloy. Two structural conditions known as slip-plane precipitation and veining were observed. "Veining" in the structure could be made to disappear and reappear by alternate solution heat treatment and age-hardening. It was concluded that the fatigue-stressing was not responsible for these structural features and the endurance limit was not reduced by it.

In attempts to detect and evaluate damage resulting from fatigue-stressing prior to the start of cracks, the impact behavior of normalized SAE X4130 steel was determined after a variety of repeated stress treatments. The results are valuable in showing the effect of fatigue cracks on impact resistance, but they do not give any indication of damage occurring before the cracks had formed.

Damage of this kind was evaluated by determining the decrease in endurance due to stressing above the fatigue limit. In a large proportion of the tests made, a deflection method was used to detect crack formation, so that the damage measurement could be definitely limited to the pre-crack stage. The results showed that the apparent rate of damage depends on the stress history. If the prestress is higher than the test stress, the damage occurs rapidly at first, then more slowly. The reverse is true if the damage is inflicted at a stress lower than that used to measure it.

## INTRODUCTION

Fatigue is one of the most important factors contributing to mechanical failure in service of highly stressed structural members of aircraft. It is apparent that the metal is being damaged throughout the period of fatigue-stressing; but the damage cannot be detected until visible cracks have formed, and when this occurs the life remaining before failure is short. For several years a research project at the National Bureau of Standards has been directed toward learning more about the damage occurring in the pre-crack stage of fatigue of metals. This is the final report on the project and includes both previously published material and new results. Part I is a recapitulation of data of reference 1, and in part II-A the previously published data of reference 2 are reconsidered in light of the new data on the same material which are presented in part II-B.

This study was conducted at the request of and with financial assistance from the National Advisory Committee for Aeronautics.

## I. EFFECT OF SERVICE STRESSES ON 25S ALUMINUM ALLOY

## A. Effect of Repeated Stress on Impact Resistance

Loss in resistance to impact has already been used by Honda and Oshiba (references 3 and 4) to measure fatigue damage. Oshiba showed a close correlation between the growth of fatigue cracks and the decrease of impact resistance in annealed carbon steels. Davidenkow and Schewandin (reference 5) found a decrease in the strength of annealed carbon steel at low temperature following repeated stress above the fatigue limit. Their work is of special interest because they found immediate lowering of the breaking strength during very early stages of the fatigue process before any fatigue crack could be discovered on the faces of the fractures.

From consideration of such results it seemed worth while examining the effects of repeated stress on the impact resistance of aluminum alloy 25S-T, particularly at a low temperature. Preliminary notched bar tests on material as received, showed that the impact resistance increased as the temperature was decreased down to  $-78^{\circ}\text{C}$ .

Haigh axial loading machines were used for the fatigue-stressing. The reduced sections of the specimens were cylindrical so as to provide material as nearly homogeneous in stress history as could be arranged. Substandard Charpy and Luerssen-Green torsion impact specimens were machined from the reduced sections in such a way as to contain no visible fatigue cracks.

The various repeated stress treatments prior to impact tests are described in table I. The results of the impact tests are summarized in table II. Detailed results of one of the five sets of tests are shown in figure 1.

It was concluded that for material not containing a fatigue crack located so as to be involved in the impact fracture, the impact resistance of alloy 25S-T was unimpaired by repeated stresses below or above the fatigue limit.

#### B. Effect of Repeated Stress on X-Ray Diffraction Patterns

The advantages of nondestructiveness and applicability to localized surface elements continue to make X-ray diffraction studies of fatigue attractive; although their competency in foretelling fatigue failure has been questioned, particularly by C. S. Barrett. (See reference 6.)

The immediate purpose of this investigation was to determine what changes, if any, could be detected in the X-ray diffraction patterns of alloy 25S-T as a result of repeated stress. Iron and molybdenum radiations were used to examine Krouse cantilever rotating beam and Haigh axial loading specimens at intervals during the course of fatigue-stressing. Table III gives the record of one of the Haigh specimens which may be considered typical of the rest.

In figure 2 the photograms b, c, and d were all obtained by exposing the same spot to the X-ray beam, an attempt being made to lock the specimen in the same position for each exposure. All the patterns of figure 2 were obtained from areas several centimeters from the point where a fatigue crack ultimately appeared. These patterns showed no definite change as a result of repeated stress above the fatigue limit. They were the same in general appearance as many others taken on unstressed material.

It is evident that the X-ray diffraction patterns did not indicate whether or not the alloy 25S-T had been damaged

by repeated stress. If a series of patterns had been obtained at various stages of the fatigue process by directing the beam at the exact spot where a fatigue crack eventually occurred, then a different result might have been obtained. Such technique is in common use on test specimens, but for the inspection of large service members hundreds of diffraction patterns would be needed to make sure that every likely spot had been examined. Such a procedure does not seem practical.

### C. Effect of Repeated Stress on the Microstructure

The terms "slip-plane precipitation" and "veining" connote quite unrelated structural conditions in aluminum alloy 25S-T. Although there was no a priori reason for regarding these structural features with suspicion, the fact that they were prominent in the microstructure of failed propeller blades prompted a study of their origin and probable significance, especially in relation to fatigue-stressing.

The appearance of slip-plane precipitation in a propeller blade of 25S-T aluminum alloy is shown in figure 3. Many of the individual grains are crossed by intersecting families of parallel lines. The micrograph of figure 4 shows that each individual line consists of a series of discrete particles.

Identification of the crystallographic planes bearing these particles was made on several large crystals found in sections through a propeller blade. Photomicrographs of the polished and etched sections were used to establish the directions of the rows of precipitated particles with respect to reference scratches. The crystal orientations were then determined from back reflection X-ray patterns.\* In all cases, intercepts of octahedral planes on the plane of polish were found to line up with the rows of particles. This, coupled with the fact that no more than four directions of the rows of particles were found in any one of the large number of grains examined, indicates clearly that the precipitation had occurred on octahedral planes.

The question immediately arising is whether or not the slip-plane precipitation is a result of service stresses and

---

\*The valuable assistance of H. C. Vacher, Metallurgist, National Bureau of Standards, is acknowledged in this phase of the work.

whether the condition is detrimental to the material, particularly in its resistance to repeated stress. In a study of the fatigue characteristics of lead cable sheath, Townsend (reference 7) concluded that structural changes occurred in an antimony-lead alloy as a result of the service conditions, primarily of the stresses, and that these changes had an important bearing on the subsequent behavior of the metal as a whole. In that case, the change which consisted essentially of the precipitation from solid solution of the antimony was confined principally to the grain boundaries. The possibility of a similar occurrence in the present case was examined.

Many different attempts to produce slip-plane precipitation in 25S-O, 25S-W, and 25S-T alloys by deformation and repeated stresses failed. Likewise, deformation of the 25S-O, or annealed alloy, followed by aging at elevated temperatures failed to produce slip-plane precipitation.

It was found that if the solution heat treated alloy (25S-W) was plastically deformed by moderate amounts in any of a large number of ways and then aged at an elevated temperature - for example,  $143^{\circ}\text{C}$  for a sufficient time, usually about 17 hours - the alloy then contained copious amounts of slip-plane precipitation. Fatigue specimens of 25S-W stressed to failure showed no evidence of slip-plane precipitation until after aging at elevated temperatures. Solution heat treatment followed by age-hardening in the usual manner was sufficient to produce the effect, without other stress treatments, particularly near corners and edges where quenching stresses were expected to be the greatest.

The results of determinations of fatigue strengths of 25S-T samples containing little and much slip-plane precipitation revealed no marked difference between the two, but if anything a slight superiority of the material containing much slip-plane precipitation.

It was concluded, therefore, that the existence of this structural condition in the material was not an indication of fatigue damage.

Experiments on veining such as shown in figure 5 in alloy 25S were sufficient to show that this condition could be suppressed and restored repeatedly by solution heat treatment and age-hardening, respectively, and that the condition offers no promise of being useful as an indication of fatigue damage.

## III. EFFECT OF SERVICE STRESSING ON Cr-Mo STEEL

### A. Effect of Fatigue-Stressing on Impact Resistance

As a possible means of detecting and evaluating damage in steel resulting from fatigue-stressing, the impact resistance of the stressed metal was determined in supplementary tests of specimens which had been fatigue-stressed short of fracture. The impact behavior of normalized SAE X 4130 steel was studied following fatigue-stressing under a variety of conditions of stress amplitude, mean stress, stress concentration, stress distribution, and temperature during stressing. Comparative data were secured for a variety of impact testing temperatures ranging from room temperature to  $-78^{\circ}\text{C}$ .

Tests made with Krouse rotating cantilever specimens stressed below the fatigue limit and subsequently broken in transverse impact showed no loss of impact resistance as compared to specimens in the as-received condition either at room temperature or  $-78^{\circ}\text{C}$ . Similarly, negative results were obtained with smooth specimens fatigue-stressed by axial loading (Haigh machine) when tested in tensile impact at room temperature and with smooth specimens fatigue-stressed transversely as rotating beams (R. R. Moore machine) when they were tested in tensile impact at room temperature and  $-33^{\circ}\text{C}$ .

None of the specimens stressed above the fatigue limit by equal tensile and compressive axial loading showed any loss in impact resistance unless surface cracks were present. The tests leading to this conclusion were as follows:

Notched specimens having a nominal fatigue limit of  $\pm 26,000$  psi were stressed as rotating cantilever beams for various numbers of cycles at  $\pm 40,000$  psi, then tested in transverse impact at room temperature,  $-20^{\circ}\text{C}$ , and  $-78^{\circ}\text{C}$ . The fact that a specimen had received a specific number of cycles of a given overstress was of small importance compared to the presence or absence of fatigue cracks.

Tensile impact tests of unnotched specimens which had been stressed as rotating beams or stressed in equal tension and compression by axial loading gave no indication of any loss in elongation or impact energy until surface fatigue cracks were present. Such cracks were not always found in advance of the impact test.

With both the above groups of specimens, tests were

made at room temperature and at one or more lower temperatures. In all cases, the presence of cracks could be detected as easily at room temperature as at low temperatures. For the notched specimens it was shown that, for a specific percentage loss of impact energy, a deeper crack can be tolerated at room temperature than at  $-20^{\circ}$  or  $-78^{\circ}$  C.

Specimens which were overstressed by superimposing fatigue stresses on mean tensile stresses varying from 17,400 to 77,000 psi extended plastically during the first few thousand cycles of stress, after which no further extension took place during the precrack stage of fatigue. Small decreases in elongation and tensile impact energy accompanied this initial extension, but these losses were also restricted to the first few thousand cycles of stress. No further change in elongation or impact energy took place until the advent of fatigue cracks.

The number of cracks formed during fatigue-stressing was in some cases dependent on the fineness of the surface finish, as shown by the following results. Specimens stressed either by axial loading or transversely as rotating beams<sup>1</sup> for which the mean tensile stress during the fatigue test was zero, developed not more than five cracks in any one specimen regardless of the finish used. Haigh specimens subjected to mean tensile stresses between 17,400 and 50,000 psi during fatigue-stressing developed many more cracks if the surface was finished with Aloxite than if it had the finer 4/0 polish. Haigh specimens subjected to a mean tensile stress of 77,000 psi during fatigue-stressing developed large numbers of fatigue cracks (maximum about 200) regardless of the finish used.

Specimens which had been fatigue-stressed by axial loading and had developed cracks were used to study the relationship between crack dimensions and tensile impact behavior. The cracks were measured with a traveling microscope focused on the fracture. Figure 6 shows the relationship for impact tests made at room temperature and  $-33^{\circ}$  C. between average tensile impact energy and the product of crack length times crack depth. Even the smallest cracks measured produced significant losses in impact energy and elongation. For specimens containing cracks smaller than a certain critical size the average impact energy was the same at room temperature and at  $-33^{\circ}$  C. For a specimen containing a crack

<sup>1</sup>In the succeeding discussion these types of specimens are designated as "Haigh" and "R. R. Moore", respectively.



larger than the critical size, the impact energy was less at  $-33^{\circ}\text{C}$  than at room temperature.

A number of specimens fatigue-stressed by axial loading sufficiently to produce cracks were machined to remove the surface layer containing the cracks. In each case, the tensile impact resistance of the remaining "core" specimen was slightly less than for similar specimens not fatigue-stressed. This difference was attributed mainly or wholly to the plastic extension received during the repeated stressing.

Specimens fatigue-stressed by flexure at  $-40^{\circ}$  to  $-45^{\circ}\text{C}$  showed no evidence of lowered impact resistance at either room or low temperatures, provided no detectable cracks were present in the metal.

From all of the above results it was evident that damage of the metal produced in the precrack stage of fatigue-stressing was not detected with impact tests.

#### B. Effect of Fatigue-Stressing on the Fatigue Strength of the Uncracked Steel

Since the measurements described in the preceding sections gave no promise of evaluating fatigue damage incurred during the precrack stage, it was decided to concentrate on a study of damage of the material as measured by the decrease in its fatigue strength. Such a study would be expected to yield information concerning the rate at which damage progresses at varying degrees of overstress. A considerable amount of work of this type has been done, particularly by Kommers (reference 8), but the majority of investigators have used the decrease in fatigue limit as a measure of damage. It was thought that tests based on the loss of endurance at stresses above the fatigue limit would give a more sensitive measurement of damage and would have the advantage of giving results more applicable to service conditions. Accordingly, most of the tests described in this section were conducted in the latter way.

1. Material and Test Methods. The material used in all of these tests was chromium-molybdenum steel, SAE X 4130 (now 4130). Material from two different heats was used, that designated as M356 being used for the Haigh and unnotched R. R. Moore specimens, while M390 was used for the notched R. R. Moore specimens. Results of chemical analyses of the two heats are given:

	M356 (percent)	M390 (percent)
C	0.31	0.30
Mn	.55	.50
P	.015	.007
S	.020	.011
Si	.21	.19
Cr	.86	.89
Mo	.19	.31
Ni	.06	.10

The material was normalized prior to machining by air cooling from 1625° F. The average mechanical properties of several specimens of material M390 are given below. The tensile specimens were of conventional design with a reduced section 0.313 inch in diameter.

Yield strength (0.2-percent offset), psi	62,500
Ultimate tensile strength, psi	104,200
Elongation in 1 inch, percent	27
Reduction of area, percent	57
Hardness-Rockwell B	90

The smooth (unnotched) specimens used in both the rotating beam and axial loading tests had minimum sections 0.200-inch diameter with an outline sweep radius of  $9\frac{7}{8}$  inches. The notched specimens had a cylindrical test section 0.35-inch diameter, into which was cut a semicircular circumferential notch 0.05 inch deep and 0.05-inch radius. The stresses listed for the notched specimens were calculated on the minimum diameter of 0.25 inch without regard to stress concentration. The smooth specimens were polished by hand with Alexite paper, the direction of polishing being parallel to the axis of the specimen. The notches in other specimens were finished with a copper wire, slightly smaller in diameter than the notch, charged with a slurry of No. 302 emery in water. The specimens were rotated slowly in a lathe while the wire, held at right angles to the axis of the specimen was rotated rapidly. In this way the fine polishing scratches at the bottom of the groove were substantially parallel to the axis of the specimen.

The Haigh testing machines used in conducting the tests for which the specimens were stressed by axial loading were operated at a frequency of 2400 cycles per minute, the mean stress being held constant at 10,000 psi tension. The smooth specimens were tested in Moore rotating beam machines at

1750 rpm; whereas the companion notched specimens were tested at 3600 rpm, most of them in a machine with which great care had been taken to minimize vibration.

In all cases of a group of results obtained under identical conditions, the median value was taken as representative of the endurance of the group. This was thought to be a more representative value than the average, as it is less affected by an occasional excessively divergent value, and it may be determined in cases where some elements of the group cannot be expressed numerically, but are known to lie in a certain range. For example, if in determining the endurance at a given stress, only one specimen did not fail, the average endurance of the group would be infinite; whereas the median value would be finite.

2. Unnotched specimens stressed by axial loading.— The endurance of unnotched specimens was determined at 83,000 psi stress range (31,500 psi compression to 51,500 psi tension) and at 84,000 psi stress range (32,000 psi compression to 52,000 psi tension). Specimens were then stressed for various cycle ratios<sup>1</sup> at one of these values of stress range and tested to failure at the other. The damage was measured by the change of endurance from that of the specimens which had not been prestressed, a negative value of the damage indicating that the endurance was greater after prestressing. The results are shown in figures 7 and 8 and in table IV.

In the table, the column headed SIQ is the semi-interquartile range<sup>2</sup> of each group of results. Both the damage and the semi-interquartile range are expressed as percent of the original endurance at the test stress. The latter is a measure of the dispersion of the individual values which expresses the same limits relative to the median as the probable error expresses relative to the average. The SIQ ranges for the results of the axial loading tests are large, so it is not surprising that the points of figures 7 and 8 are widely scattered. It is difficult to draw conclusions from these results, but it appears that there was improvement in

<sup>1</sup>The term, cycle ratio, as used here, designates the ratio of the number of cycles run at the prestress to the total number of cycles which would cause failure at this stress.

<sup>2</sup>The middle number of a series arranged in order of magnitude is the median. The middle one of the numbers that lie below the median is the lower quartile, the middle one of those above is the upper quartile. Half the difference between the upper and lower quartiles is the semi-interquartile range.

the endurance at 84,000 psi due to prior stressing at 83,000 psi stress range. It is evident that very many more specimens would have been required to obtain reliable approximations to the true damage curves.

3. Unnotched specimens stressed as rotating beams.— A testing program similar to that presented in the preceding section was conducted with R. R. Moore rotating beam machines. The fatigue limit was  $\pm 49,500$  psi, and the two stresses chosen for prestressing and testing were  $\pm 55,000$  psi and  $\pm 65,000$  psi. The results are shown in figures 9 and 10 and table V.

It will be noted from the tables that the dispersion in these tests, as measured by the SIQ range was much less than in the axial loading tests, and the results may be expected to be correspondingly more reliable. Figure 9 shows definitely that when the prestress was higher than the test stress the damage occurred more rapidly at first. The opposite tendency is indicated in figure 10. In this case the prestress was lower than the test stress. The marked improvement obtained in these tests is surprising and the results are open to some question because of the small number of specimens used to establish the points. An attempt to verify this improvement with a few specimens of a different heat of the same steel was unsuccessful. The stresses used were the same, and the value obtained is represented by the point labeled U on figure 10.

In addition to the above tests in which damage was measured by the decrease in endurance by prestressing at stress values above the fatigue limit, a group of specimens was also run to determine the damage as measured by the decrease in the fatigue limit due to prestressing at  $\pm 65,000$  psi. The results of these tests are listed in table VI and plotted in figure 9.

4. Notched specimens stressed as rotating beams.— The tests described in the preceding sections resulted in several conclusions regarding the requirements for satisfactory methods for evaluating fatigue damage. First, it is obvious that the axial load tests resulted in so much scatter that satisfactory precision could not be obtained with any reasonable number of specimens. Second, even with the smaller dispersion obtained in the rotating beam tests, an average of about eight specimens would be required to give significant results for each condition. Third, the evaluation of damage by running tests to fracture is limited to cycle ratios sufficiently small so that the chance of crack formation during prestressing

is negligible; otherwise some specimens would be included in which the damage was dependent only on the size of an initial fatigue crack rather than on the effect of prestressing.

The methods followed in the final stage of the study of fatigue damage were chosen in light of these conclusions. In order to guard against cracking during prestress it was necessary to have a means of detecting fatigue cracks at an early stage without stopping the test. Such a method was developed, based on the fact that the deflection of a rotating beam specimen under constant load increases when a crack forms. The apparatus and technique used to detect and measure this deflection have already been described in detail. (See reference 9.) The method used was essentially as follows: One of a pair of contacts was fastened to the specimen end of a bearing housing on the R. R. Moore machine, the other contact being carried on a micrometer screw mounted on the bed of the machine. The contacts operated a signaling device through a tube circuit, so the position of the upper contact could be determined by raising the lower contact and noting the reading of the micrometer screw when the circuit was closed.

In order to get the best results with this apparatus it was necessary to mount the fatigue testing machine on springs to minimize vibrations from extraneous sources. Also, no specimen was used which caused excessive vibration when the machine was running. With these precautions it was possible to set the contacts 0.001 to 0.002 mm apart, so that a deflection of this amount would operate the signal. The deflection is a function of the size of crack, and the criterion of failure chosen was a deflection of 0.005 mm. As shown in reference 9, this corresponds to a crack area about 12 percent of the original cross section. The specimens were actually run until the deflection had increased to 0.01 mm in order to make certain that the deflection was due to a crack, but the data in the next section are based on the number of cycles run before the specimen deflected 0.005 mm. This number is referred to as  $N_c$ .

Tests were conducted in the conventional manner on a group of notched specimens to determine the S-N curve and the fatigue limit (tests to fracture). Four stresses between the fatigue limit and the yield strength of the steel were chosen to be used in the investigation. The fatigue limit of the notched specimens was found to be 39,000 psi and the four stresses chosen were 42,000, 48,000, 54,000 and 60,000 psi.

Tests were then made to determine  $N_c$  at each of the 4 chosen stresses. At least 10 specimens were tested at each stress, and the median of each group was used as the value of endurance at that stress.

Since the scatter of the results was not uniform in the 4 groups, it was necessary to test more specimens in some cases than in others in order to obtain approximately the same precision for each value of  $N_c$ . The number of tests in each group ranged from 11 to 17 for this reason.

The values of  $N_c$  (the number of cycles to form a crack of definite size) for each selected stress are listed below:

±42,000 psi	for	$963 \times 10^3$ cycles
±48,000 psi	for	$264 \times 10^3$ cycles
±54,000 psi	for	$93 \times 10^3$ cycles
±60,000 psi	for	$44 \times 10^3$ cycles

In the next stage of the investigation each specimen was first stressed for a predetermined number of cycles at one of the four chosen stresses; then the stress was changed as given below and the number of cycles to failure determined. Comparison of this value with the above median values gave a measure of the damage caused by the prestressing. Four different combinations of prestress and test stress were used as follows:

<u>Prestress</u>	<u>Test stress</u>
±42,000 psi	±48,000 psi
±54,000 psi	
±48,000 psi	±54,000 psi
±60,000 psi	

Thus, there was one prestress higher and one lower than each test stress. For each of the above combinations, tests were made with the prestressing carried to 10, 25, 50, 75, and 90 percent of the median value of  $N_c$ . The number of tests made for each amount of prestress was between 6 and 10 depending on the scatter of the individual values. The median was again used as the value representative of each group and the values are listed in table VII. The variation of damage with percent prestress is shown graphically in figures 11 and 12 for a test stress of ±48,000 psi, and in figures 13 and 14 for a test stress of ±54,000 psi. In the graphs the broken lines join the upper and lower quartile points of each group of values and thus give an indication of the scatter of

the data. The curves from figures 11 to 14 are combined in figure 15 for comparison.

In the test groups in which prestressing was carried to 75 and 90 percent of the endurance, some specimens failed before the prestressing was completed - that is, the damage was greater than 100 percent. This caused no difficulty in determining the median, although it did make the comparison of precision between the groups more uncertain.

While the results of the damage tests as shown in figure 15 are not directly comparable with those obtained with smooth specimens, there are certain similarities. The tendency with both types of specimen was for the curve representing a prestress above the test stress to lie above the 45° line. The opposite tendency was noted when the magnitude of the prestress was below that of the test stress. (The 45° line may be considered as the damage curve for a prestress equal to the test stress.)

In order to provide a basis of comparison with the results on fatigue damage reported by others (usually based on the fatigue limit), some tests of this type were conducted with two values of prestress,  $\pm 42,000$  and  $\pm 60,000$  psi. The effect of various amounts of prestressing on the fatigue limit subsequently determined by fracture tests is shown in figure 16 and table VIII. The number of cycles of prestress used for the 75- and 90-percent cycle ratios was the same as the number used in the previous phase of the investigation, but a correction was made in determining the cycle ratios represented by these amounts of prestressing. The method of making this correction will be shown for the case of the highest cycle ratio at  $\pm 42,000$  psi. The median  $N_c$  for this stress was  $963 \times 10^3$ . When it was desired to prestress a group of specimens to 90 percent of this value, or  $867 \times 10^3$  cycles, some of the specimens failed before prestressing was completed. Only those which did not fail in prestressing could be used for the determination of fatigue limit; so this determination was not truly representative. Therefore, in the original series of values of  $N_c$ , the median of all values greater than  $867 \times 10^3$  was taken as being representative of the specimens which were used to determine the fatigue limit after prestressing. The cycle ratio as plotted in figure 16 is based on this second median ( $1057 \times 10^3$  cycles), and is consequently less than 90 percent. A similar correction was made for the 75-percent prestress at  $\pm 42,000$  psi, and for the 90-percent value at  $\pm 60,000$  psi. The corrected values of cycle ratio at  $\pm 42,000$  psi were 68

and 80 percent; at  $\pm 60,000$  psi, the highest value was 77 percent.

The apparent repair of damage during stressing at  $\pm 42,000$  psi is surprising, and should be verified by additional work. Since each point of figure 16 represents only five specimens, the rise in the fatigue limit may possibly be due to variations in the specimens.

In order to make the data on the effect of prestressing on endurance ( $N_c$ ) (fig. 15) more directly comparable with those on the effect of prestressing on fatigue limit (fig. 16), an attempt was made to determine the fatigue limit of cracked specimens. The accurate calculation of stress on a specimen containing a fatigue crack is virtually impossible because of the irregular and unpredictable shape of the crack. A rough estimate of the increase in stress with spreading of the crack was made by assuming the stress inversely proportional to the ratio of uncracked area to original area.

The specimens used for this determination had deflected 0.010 mm in the fatigue test. This corresponded to a crack area equal to 17 percent of the original minimum section and the fatigue limit of the cracked specimen was found to be  $\pm 23,500$  psi. In figure 17 the data of figure 16 have been replotted with the damage expressed as percentage of the damage caused by a crack of this area ratio. The straight line drawn through the data points for 60,000 psi was determined by the method of least squares.

Figure 18 shows the S-N curves for specimens with three types of stress concentration: smooth (zero concentration), notched, and cracked (maximum concentration). The points marked X or + in figure 18 are the results from cracked specimens having crack areas other than 17 percent. It will be noted that the value for a specimen having an area ratio of 50 percent lies very far above the 17-percent ratio curves while the values for specimens having a 12-percent ratio are in the same range or lower. This suggests that the stress concentration at high stresses is less for large cracks than for small cracks. Much more experimental work would be required before any general statement could be made with certainty.

In table IX are shown the values of stress concentration factors given by the ratios of the fatigue limits of the specimens under three conditions of stress concentration.



Almen (reference 10) has shown that the slope of the falling part of the S-N curve increases with increasing stress concentration. If the slope of the falling part of the S-N curve is a measure of effective stress concentration, then the ratios of the slopes of the three lines of figure 18 should give the same values for these factors. The slopes and ratios are given in table IX, and the agreement with the factors determined from the fatigue limits is satisfactory. The value of theoretical stress concentration factor given in the table for the notched specimen was calculated from a formula given in reference 11.

### CONCLUSIONS

1. The possible deleterious effect of long-continued fatigue-stressing short of failure was studied on two metals used in aircraft construction. These were 25S aluminum alloy and X4130 chromium-molybdenum steel.

2. Prolonged fatigue stressing prior to the formation of cracks did not cause embrittlement (as measured by resistance to impact) in either metal. After cracks had formed, the loss in impact resistance was a function of the size of the cracks.

3. In the case of X4130 steel it was found that the embrittling effect of fatigue cracks was greater at low temperature than at room temperature.

4. Study of X-ray diffraction patterns and microstructural features of 25S aluminum alloy showed that these are not competent to detect fatigue damage.

5. Measurement of specimen deflection in a rotating beam fatigue test provides a satisfactory method for the early detection of fatigue cracks without stopping the test.

6. The decrease in endurance at stresses above the fatigue limit was a more sensitive measure of fatigue damage than was the decrease in fatigue limit.

7. The apparent rate of damage by fatigue-stressing short of crack formation was dependent on the relationship between the stress at which the damage was done and that used to measure it.

8. If the prestress was greater than the test stress, the damage occurred rapidly during the first part of the test, then more slowly. The reverse was true if the prestress was less than the test stress. Thus, in a machine which must endure overstress, it would be beneficial to avoid relatively high stresses during the early part of its life.

9. The damage as measured by reduction of the fatigue limit occurred at a uniform rate when the stress was far above the fatigue limit. When the stress was only slightly above the fatigue limit, little damage occurred up to 80 percent of the precrack endurance.

10. Because the scatter of fatigue test results is inherently large, it is necessary to run a sufficiently large number of tests under each set of conditions so that the dispersion will not be larger than the effect of changing conditions. This consideration has not received sufficient attention in much fatigue testing, including some of the work on this project.

11. The slopes of the falling part of the S-N curves for the same material in smooth, notched, and cracked specimens showed approximately the same (stress concentration) ratios as the fatigue limits.

National Bureau of Standards,  
Washington, D. C., January 6, 1945.

## REFERENCES

1. Kies, J. A., and Quick, G. W.: Effect of Service Stresses on Impact Resistance, X-Ray Diffraction Patterns, and Microstructure of 25S Aluminum Alloy. NACA Rep. No. 659, 1939.
2. Kies, J. A., and Holshouser, W. L.: Effects of Prior Fatigue-Stressing on the Impact Resistance of Chromium-Molybdenum Aircraft Steel. NACA TN No. 889, 1943.
3. Honda, K.: Theoretical Considerations on Static and Dynamic Tensile and Notched Bar Tests. The Science Reports of the Tohoku Imperial Univ., first series, Sendai, Japan, vol. 16, 1927, pp. 265-277.
4. Oshiba, F.: The Degree of Fatigue of Carbon Steels under Reversed Bendings. The Science Reports of the Tohoku Imperial Univ., first series, Sendai, Japan, vol. 26, 1937-38, pp. 323-340.
5. Davidenkow, N., and Shewandin, E.: "Über den Ermüdungsriß." Metallwirtschaft, vol. 10, pt. II, 1931, pp. 710-714.
6. Barrett, C. S.: Predicting a Fatigue Failure; Are X-Rays Competent? Metal Progress, vol. 32, 1937, pp. 677-678.
7. Townsend, J. R.: Fatigue Studies on Telephone Cable Sheath Alloys. Proc. A.S.T.M., vol. 37, pt. II, 1927, pp. 153-172.
8. Kommers, J. B.: The Effect of Overstressing and Understressing in Fatigue. Proc. A.S.T.M., vol. 43, 1943, p. 749.
9. Bennett, John A.: Early Detection of Cracks Resulting from Fatigue Stressing. NACA RB No. 4115, 1944.
10. Almen, J. O.: The Useful Data to be Derived from Fatigue Tests. Metal Progress, vol. 44, 1943, p. 254.
11. Roark, Raymond, J.: Formulas for Stress and Strain. McGraw-Hill Book Co., Inc., 2d ed., 1943.
12. Brueggeman, W. C., Mayer, M., and Smith, W. H.: Axial Fatigue Tests at Two Stress Amplitudes of 0.032-Inch 24S-T Sheet Specimens with a Circular Hole. NACA TN No. 983, 1945.

Table I - Fatigue Stressing of Specimens in Haigh Axial Loading Machine at Room Temperature Prior to Impact Tests.

(The frequency was 2,400 cycles per minute in all cases)

Mode of repeated stressing	Mean stress (lb/sq. in). tension	Stress Limits		Stress Range (lb/sq. in).	Cycles of Stress	Remarks
		Maxi-mum (lb/sq. in).	Mini-mum (lb/sq. in).			
a----	3,650	10,150	-2,850	13,000	25,000,000	Unbroken
b----	20,900	37,600	4,200	33,400	288,000	do
c----	20,900	37,600	4,200	33,400	153,000 to 480,000	Broken
d----	20,900	38,200	3,600	34,600	144,000	Unbroken
e----	20,900	38,200	3,600	34,600	288,000	do
f----	20,900	38,200	3,600	34,600	192,000 to 276,000	Broken
a.r.	0	0	0	0	0	As received

Table II. - Impact Resistance of 25ST Aluminum Alloy Previously Subjected to Fatigue Stress.

Impact test method	No. of impact specimens broken	Temperature of test (°C)	Mode of previous fatigue stress <sup>1</sup>	Notch depth (in.)	Average impact energy (ft.-lb)	Average deviation from mean (percent)	Scatter (ft.-lb)
Charpy	{ 18	25	a.r.	0.039	6.0	8.3	2.6
	{ 20	25	(a)	.039	5.7	9.3	2.0
	{ 20	25	a.r.	.005	14.6	5.1	3.4
	{ 14	25	(b)	.005	14.7	7.5	4.0
	{ 5	25	(c)	.005	15.1	7.3	2.7
Torsion	{ 18	25	a.r.	None	54.0	7.2	28.0
	{ 2	25	(a)	None	57.0	7.0	8.0
	{ 15	-78	a.r.	0.005	16.7	6.0	5.2
Charpy	{ 8	-78	(d)	.005	16.9	10.0	5.4
	{ 4	-78	(e)	.005	15.7	7.6	2.5
	{ 3	-78	(f)	.005	18.8	3.2	1.8
	{ 6	-78	a.r.	.039	8.0	15.0	3.5
	{ 6	-78	(d)	.039	6.5	21.5	4.3

<sup>1</sup>See Table I for mode of previous fatigue stress.

Table III. - Repeated Stress - X-Ray Diffraction Record of a Specimen of Alloy 25ST.

Specimen 4H4A Stress Range 4,200 to 37,600 lb/in<sup>2</sup> Tension

Date Stressed	Cycles	Date of X-Ray	Figure
2/23/38	288,000	4/27/38	2a
		4/28/38	2b
4/29/38	36,000 additional	4/29/38	2c
5/26/38	79,200 additional (failed)	6/2/38	2d

Table IV. - Effect of Prestress on Endurance for Unnotched Specimens; SAE X4130 steel, fatigue stressed by axial loading.

No. of Specimens	Test Stress psi	Prestress Range, psi	Cycle Ratio %	Endurance, 10 <sup>3</sup> Cycles	Damage %	SIQ % (a)
13	83,000 Stress Range	--	0	156	0	98
9		84,000	6	161	-3	46
6			20	60	62	69
6			40	135	13	50
7			60	46	71	45
5	84,000 Stress Range	--	0	125	0	28
6		83,000	5	157	-25	67
5			15	244	-95	77
8			46	116	7	58

(a) SIQ = Semi-interquartile range

Table V - Effect of Prestress on Endurance of Specimens of Unnotched SAE X4130 Steel, fatigue stressed as rotating beams.

No. of Specimens	Test Stress	Prestress	Cycle Ratio %	Endurance $10^3$ Cycles	Damage %	SIQ*
3	$\pm 55,000$ psi	--	0	557	0	77
4		$\pm 65,000$ psi	0.8	550	1	12
8			4	336	40	36
8			8.5	331	41	12
4			17	296	47	22
7			33	244	56	7
8			67	156	72	17
10	$\pm 65,000$ psi	--	0	60	0	25
2		$\pm 55,000$ psi	1.8	87	-45	--
3			9	55	8	10
3			18	85	-42	62
3			36	103	-72	68
4			54	15	75	28
3			72	42	30	48

\* SIQ = Semi-interquartile range

Table VI - Effect of Prestress  $\pm 65,000$  psi on fatigue limit of unnotched specimens of SAE X4130 steel stressed as rotating beams.

Cycle Ratio, %	Fatigue Limit, psi	Reduction in Fatigue Limit, %
0.8	48,500	2
8	49,000	1
33	46,500	6
67	44,000	11

Table VII. - Effect of prestress on endurance of notched specimens of SAE X4130 steel stressed as rotating beams.

No. of Specimens	Test Stress psi	Prestress psi	Cycle Ratio, %	Endurance 10 <sup>5</sup> Cycles	Damage %	SIQ* %
17	± 42,000	--	0	963	0	25
11	± 48,000	--	0	264	0	13
7		± 42,000	10	198	25.0	12.5
10			25	220	16.7	18
10			50	192	27.3	20
10			75	177	32.9	26
10			90	11	95.8	--
8	± 48,000	± 54,000	10	205	22.3	14
7			25	125	52.6	12
7			50	72	72.7	9
7			75	50	81.1	15
8			90	12	95.5	--
17	± 54,000	--	0	93	0	26
8		± 48,000	10	87	6.4	23
6			25	73	21.5	10
8			50	59	36.6	16
8			75	27	71	--
8			90	3	96.8	--
15	± 54,000	± 60,000	10	84	9.7	21
7			25	63	32.2	14
6			50	31	66.7	10
8			75	15	83.9	12
8			90	3	96.8	--
15	± 60,000	---	0	44	0	23

\* SIQ = Semi-interquartile range

Table VIII. - Effect of Prestress on Fatigue Limit of Notched Specimens of SAE X4130 Steel Stressed as Rotating Beams.

Prestress $\pm$ 42,000 psi			Prestress $\pm$ 60,000 psi		
Cycle Ratio, %	Fatigue Limit, psi	Damage, % of max.	Cycle Ratio, %	Fatigue Limit, psi	Damage, % of max.
10	39,500	-3	10	38,000	6
25	39,000	0	25	35,000	26
50	37,000	13	50	31,000	52
68	37,500	10	75	26,500	81
80	38,500	3	77	28,500	68

Table IX. - Stress Concentration Factors in Specimens of SAE X4130 Steel Stressed as Rotating Beams.

Type of Specimen	Fatigue Limit, psi	S.C.F.* from Fatigue Limit	Slope of S-N curve	S.C.F.* from Slope	Theoretical S.C.F.*
Smooth	50,000	1.0	.767	1.0	1.0
Notched	39,000	1.28	.983	1.28	1.59
Cracked, 17%	23,500	2.13	1.46	1.91	--

\* S.C.F. = Stress Concentration Factor



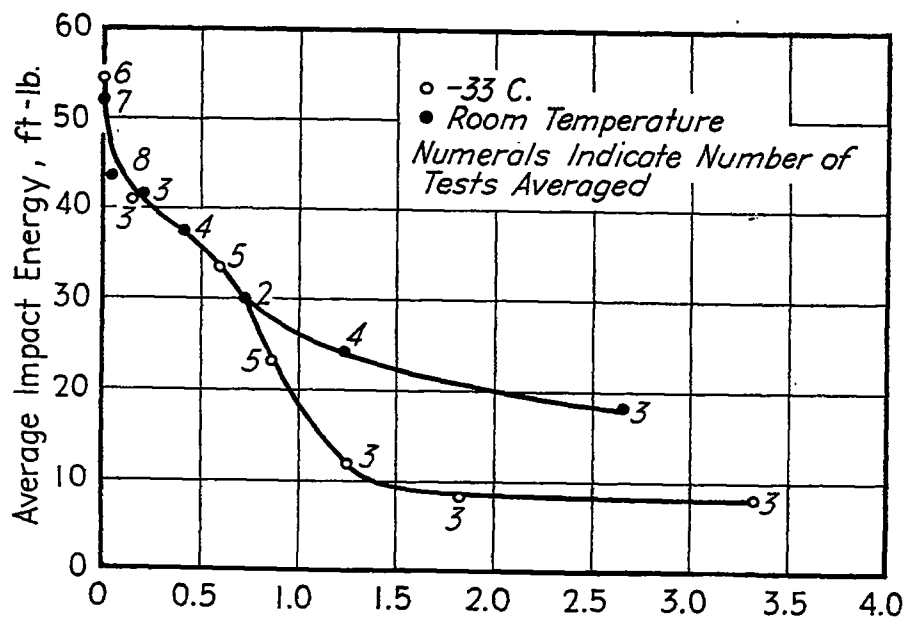
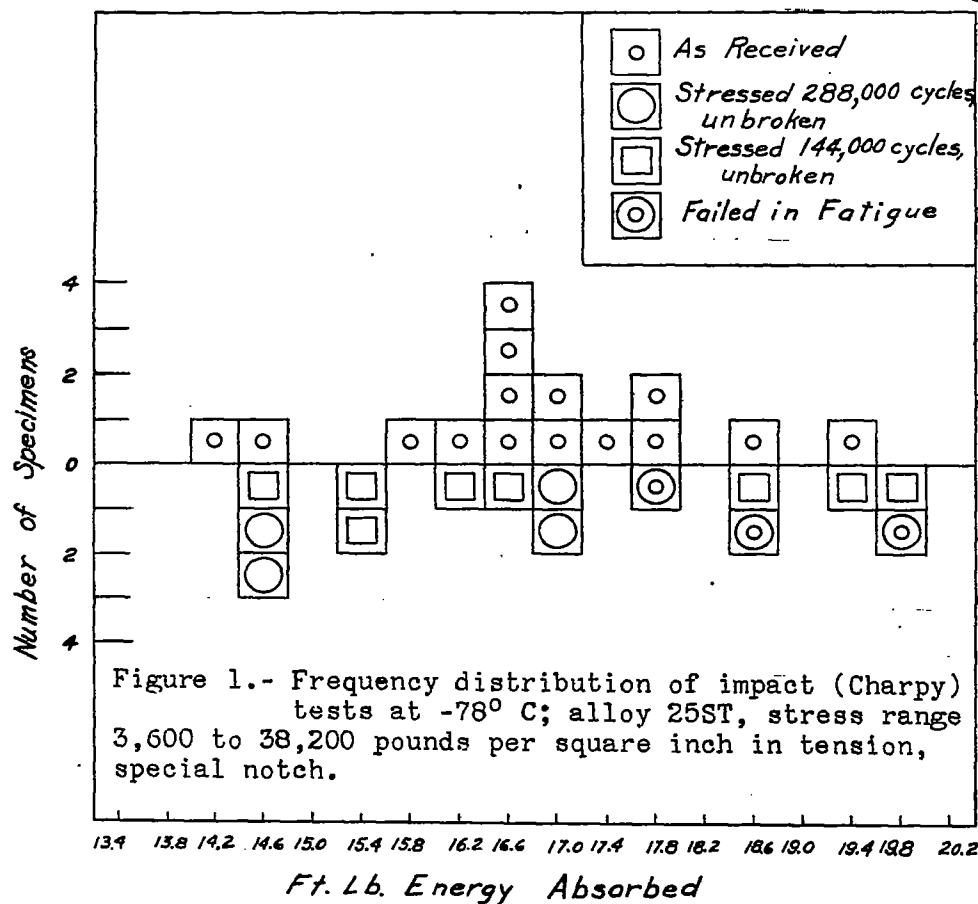




FIGURE 2.—Progressive X-ray diffraction study of surface of alloy 25ST fatigue stressed in the range 4,200 to 37,600 psi in tension. (a) and (b) 288,000 cycles, different areas being exposed to the X-ray beam. (c) 36,000 additional cycles on the same spot as (b). (d) Same spot 79,200 additional cycles resulting in fatigue failure. The crack formed several centimeters from the X-rayed spot.

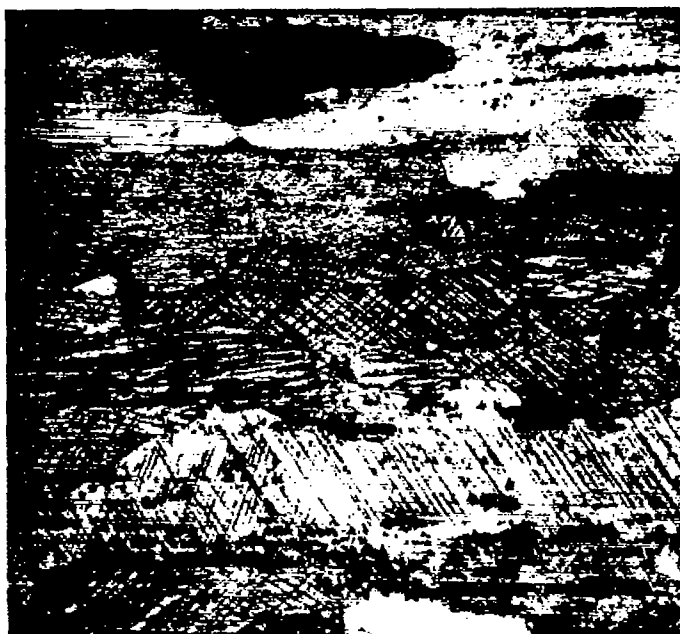


FIGURE 3.—Structural features, slip plane precipitation, in a propeller blade of 25ST aluminum alloy. The change in direction of the family of parallel lines at grain boundaries proves that the markings are not polishing scratches. Etchant: 2½% HNO<sub>3</sub>, 1½% HCl, 1% HF. × 100.

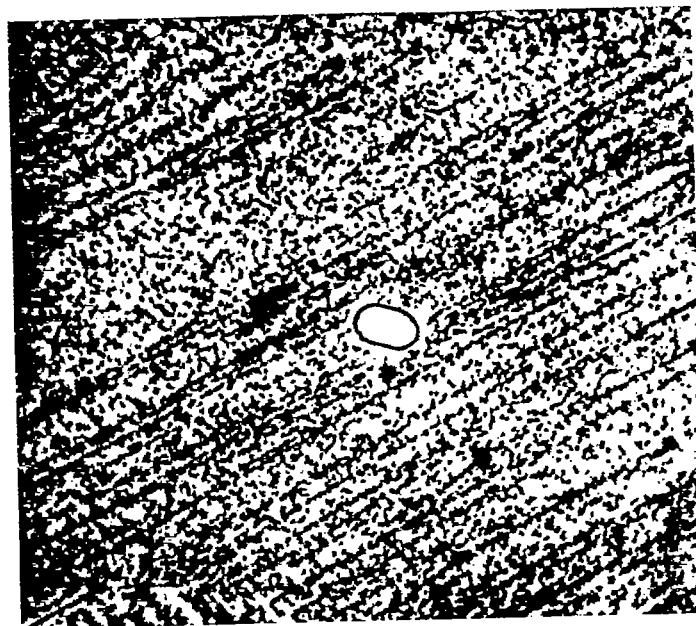


FIGURE 4.—Same structure as in previous figure, higher magnification. The rows of particles appeared as lines under low magnifications. Etchant:  $\frac{1}{2}\%$  HF.  $\times 1000$ .

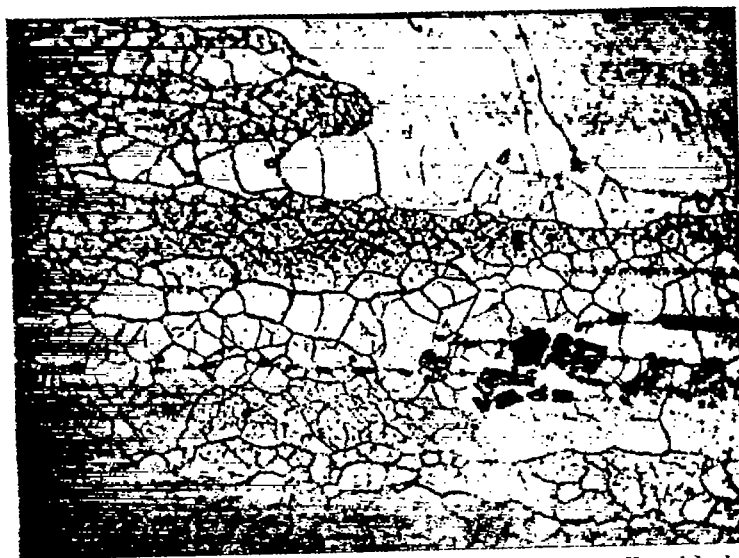


FIGURE 5.—Veining in a section of 25ST aluminum alloy propeller blade. Etchant:  $2\frac{1}{2}\%$   $\text{HNO}_3$ ,  $1\frac{1}{2}\%$   $\text{HCl}$ ,  $1\%$   $\text{HF}$ .  $\times 500$ .

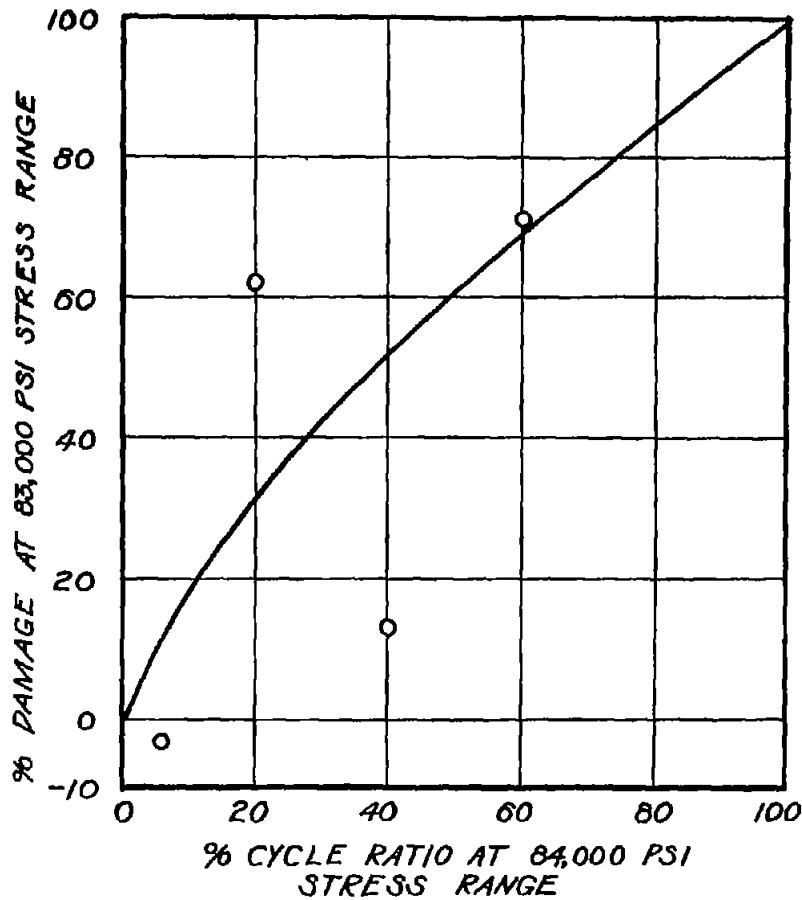


Figure 7.- Change in endurance at 83,000 psi stress range after pre-stressing at 84,000 psi stress range. Smooth, unnotched, Haigh specimens.

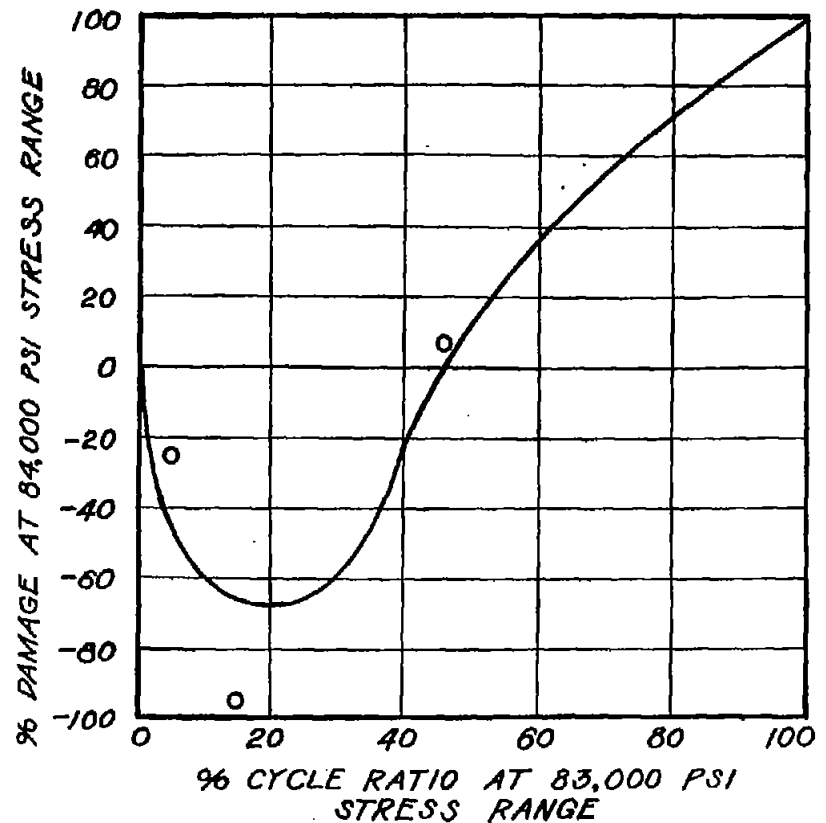


Figure 8.- Change in endurance at 84,000 psi stress range after pre-stressing at 83,000 psi stress range. Smooth, unnotched, Haigh specimens.

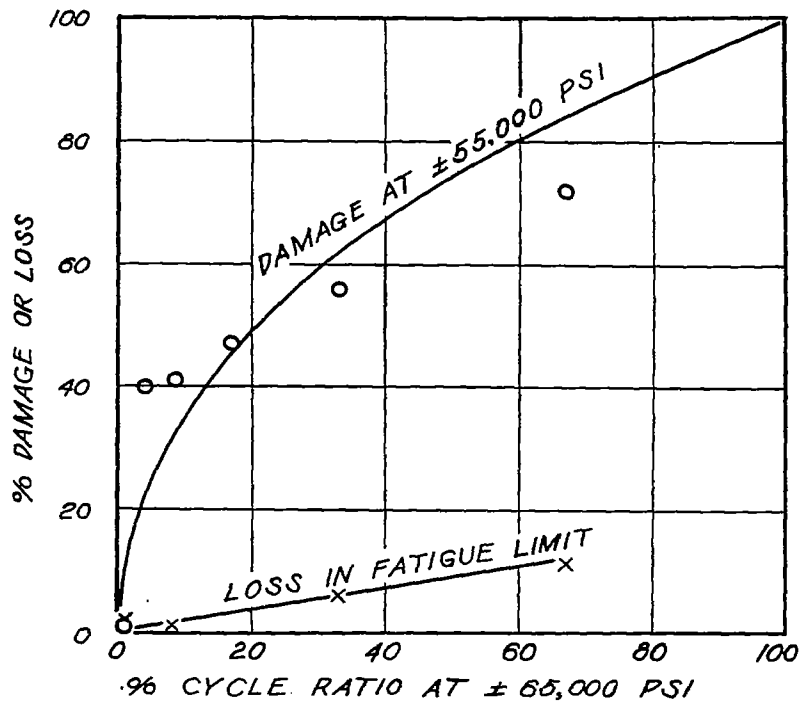


Figure 9.- Change in endurance at  $\pm 55,000$  psi and fatigue limit after prestressing at  $\pm 65,000$  psi. Smooth, unnotched, R. R. Moore specimens.

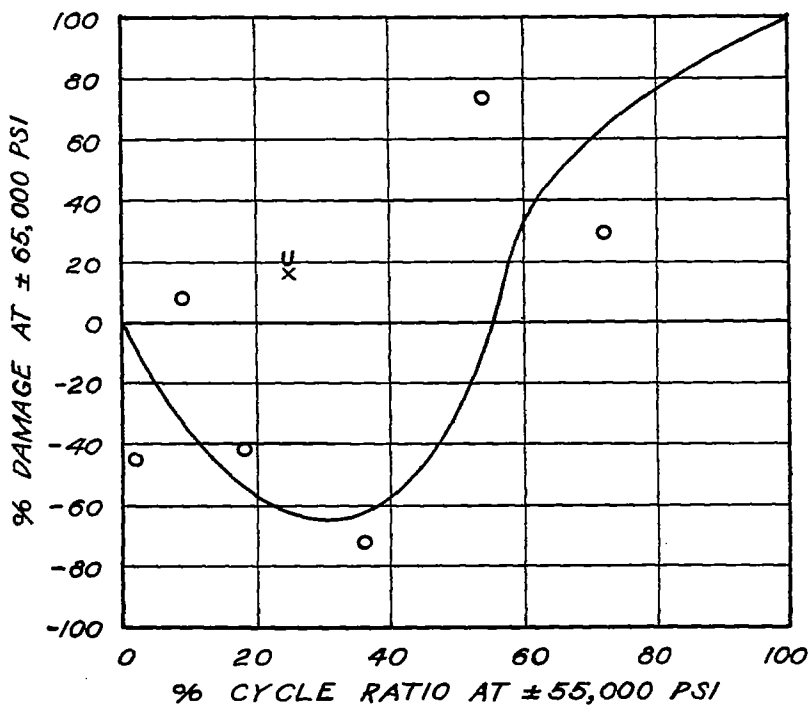


Figure 10.- Change in endurance at  $\pm 65,000$  psi after prestressing at  $\pm 55,000$  psi. Smooth R. R. Moore specimens.

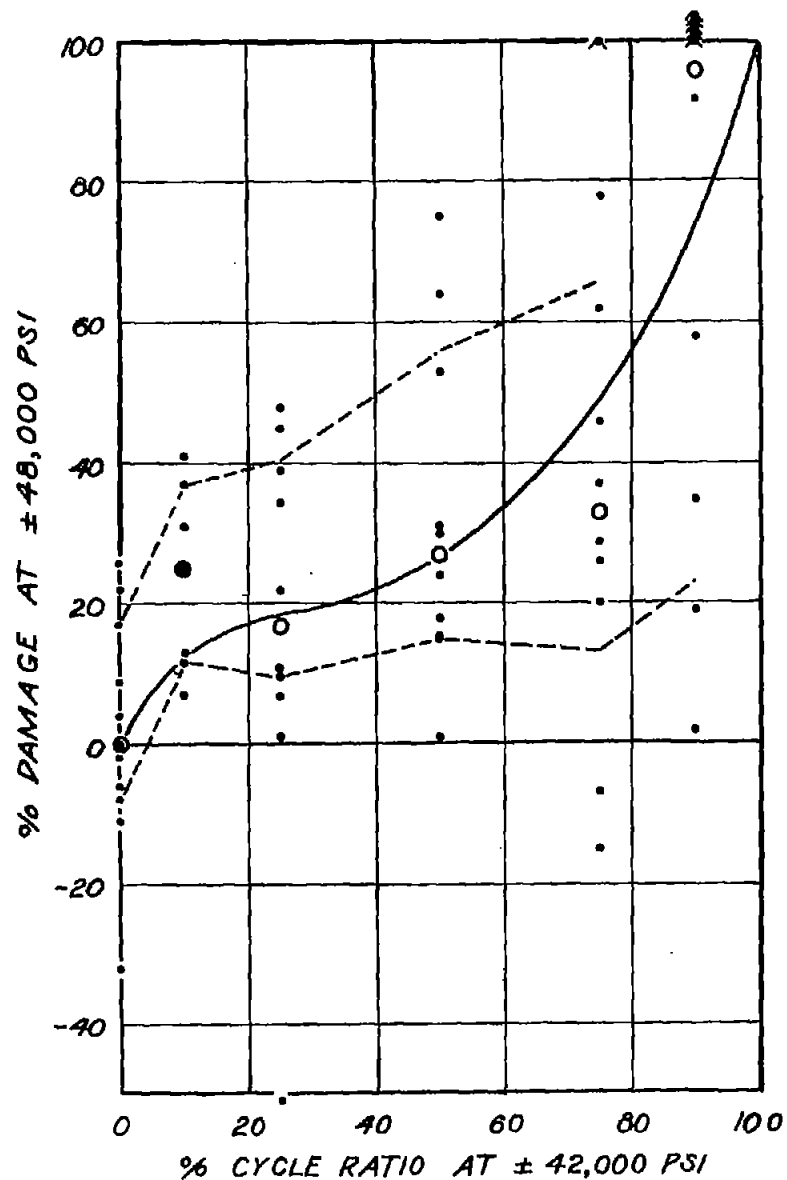


Figure 11.- Change in endurance at  $\pm 48,000$  psi after prestressing at  $\pm 42,000$  psi. Notched R. R. Moore specimens.

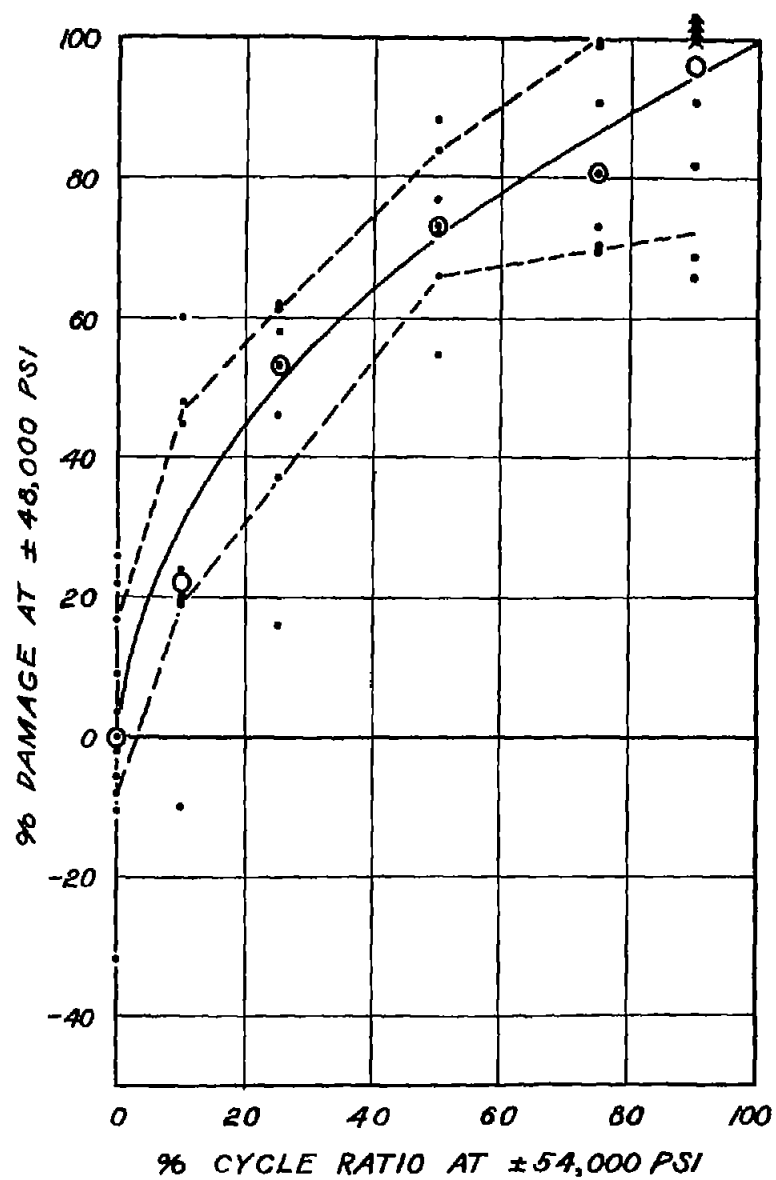


Figure 12.- Change in endurance at  $\pm 48,000$  psi after prestressing at  $\pm 54,000$  psi. Notched R. R. Moore specimens.

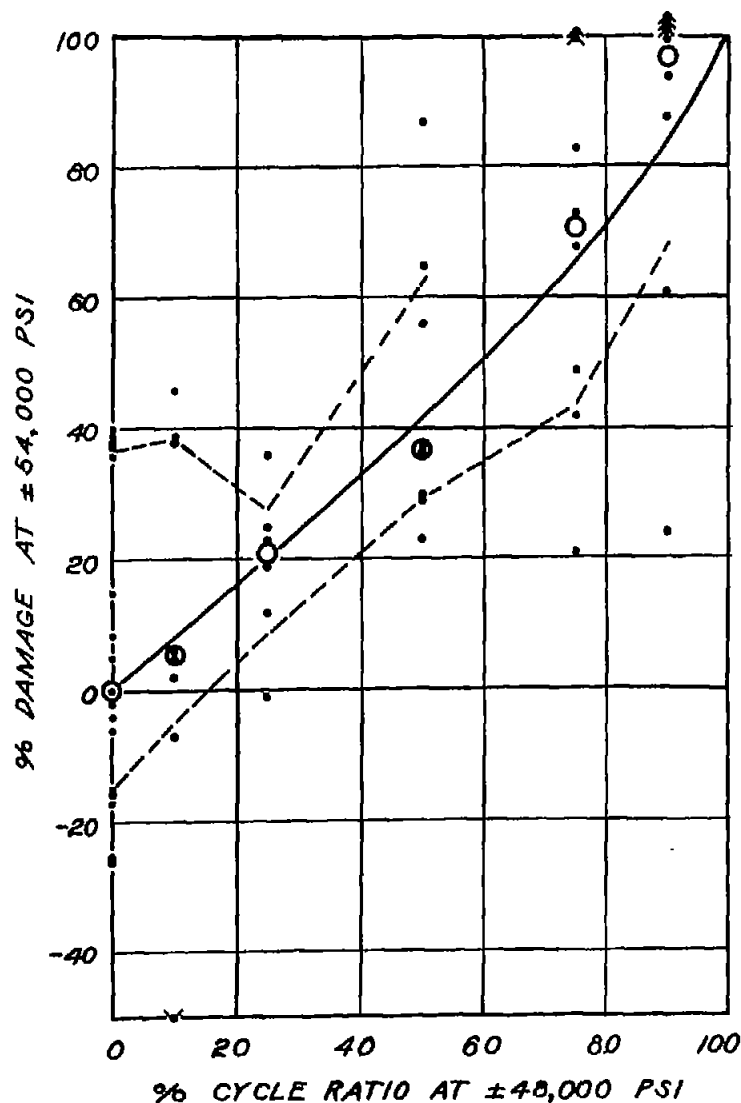


Figure 13.- Change in endurance at  $\pm 54,000$  psi after prestressing at  $\pm 48,000$  psi. Notched R. R. Moore specimens.

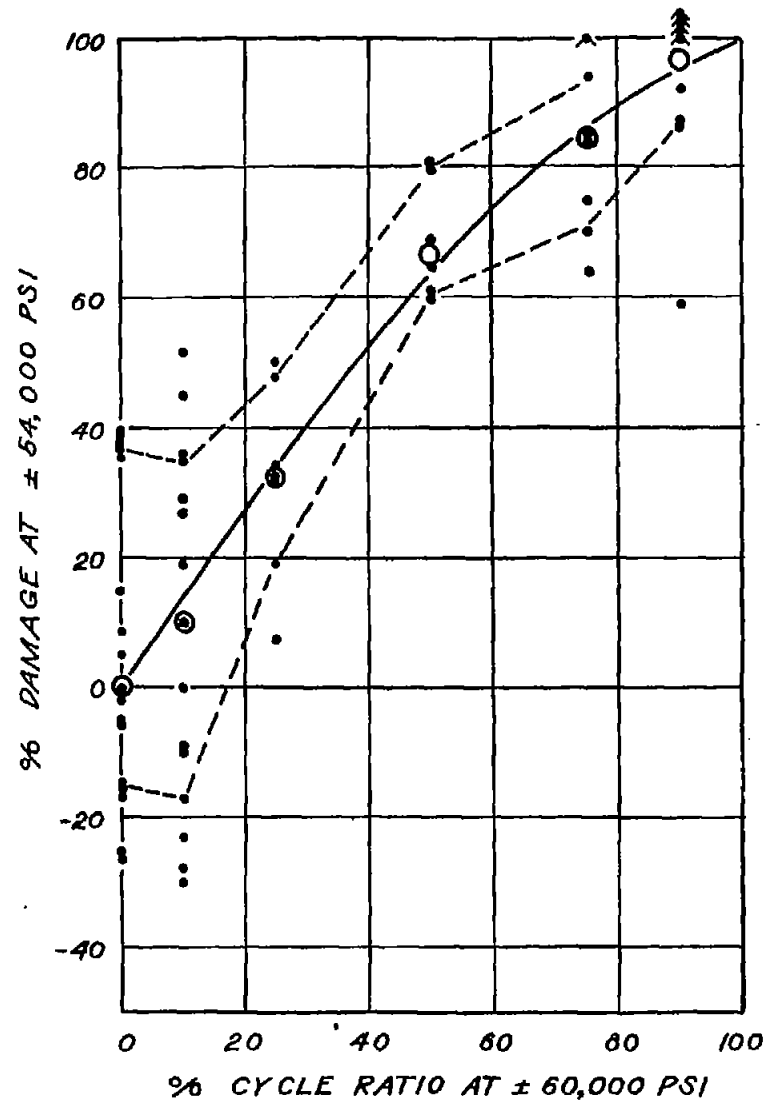


Figure 14.- Change in endurance at  $\pm 54,000$  psi after prestressing at  $\pm 60,000$  psi. Notched R. R. Moore specimens.

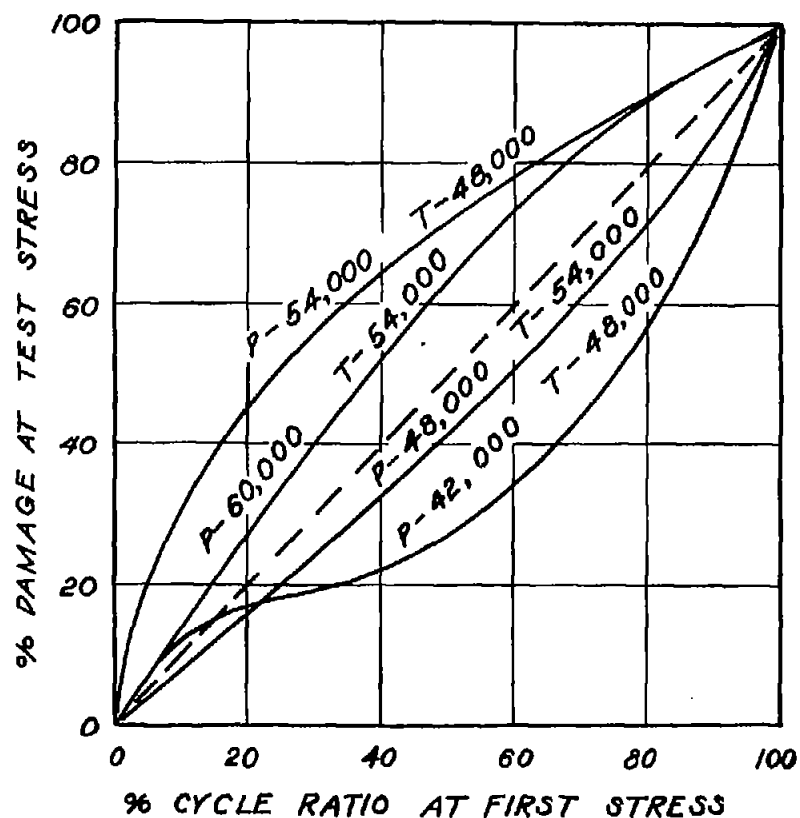


Figure 15.- Effect of prestress on endurance ( $N_c$ ). Curves from figures 11 to 14. P = prestress in psi; T = test stress in psi.

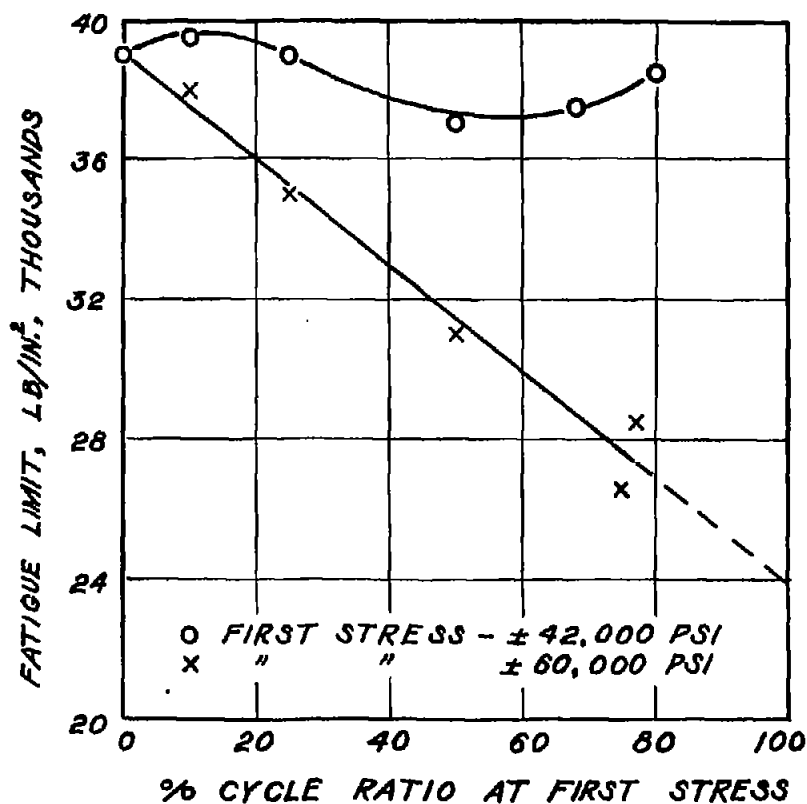


Figure 16.- Effect of prestress on fatigue limit. Notched R. R. Moore specimens.



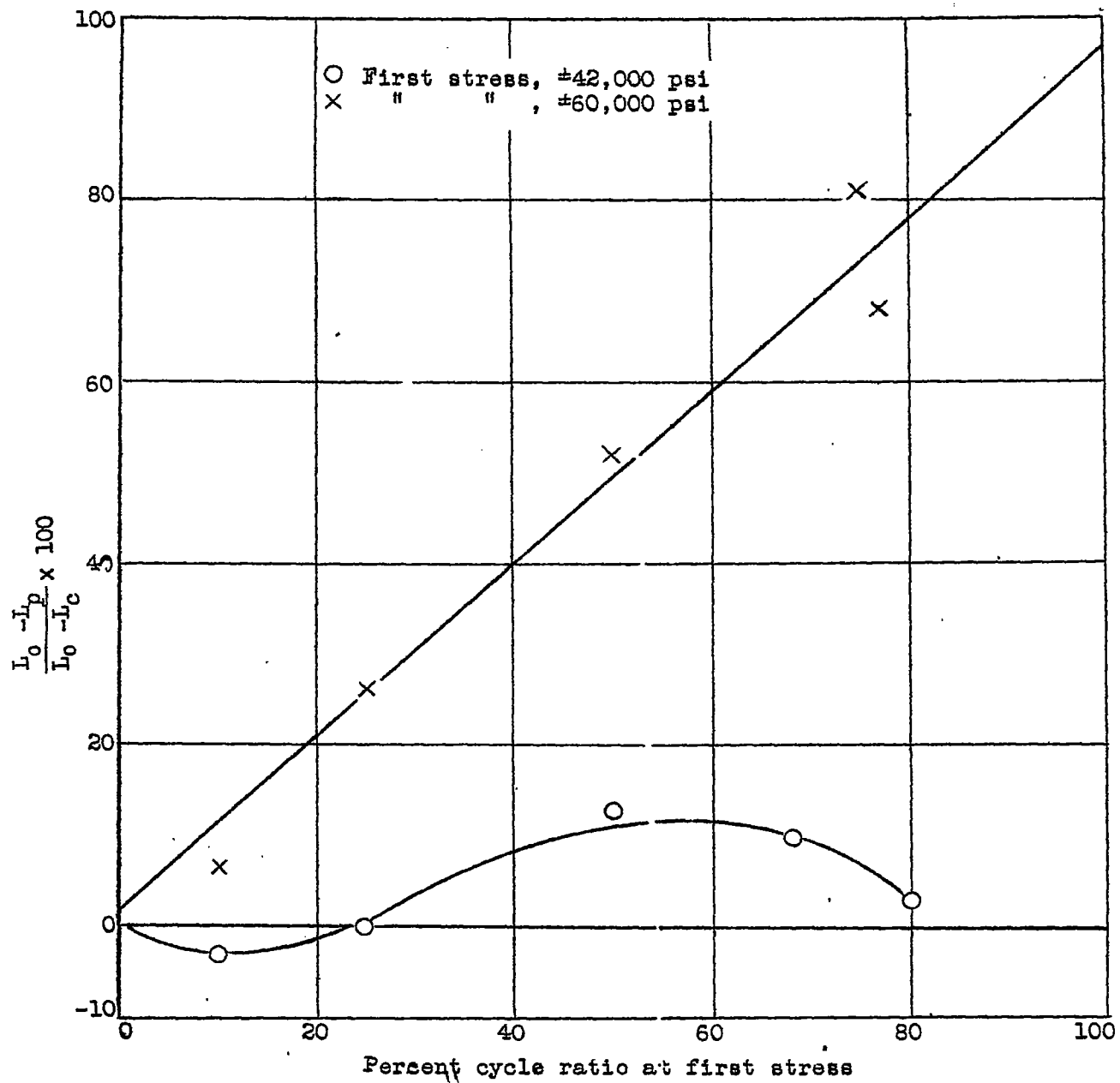


Figure 17.- Effect of prestress on fatigue limit.  $L_0$  = fatigue limit of original specimen.  $L_p$  = fatigue limit of prestressed specimens.  $L_c$  = fatigue limit of cracked specimen.

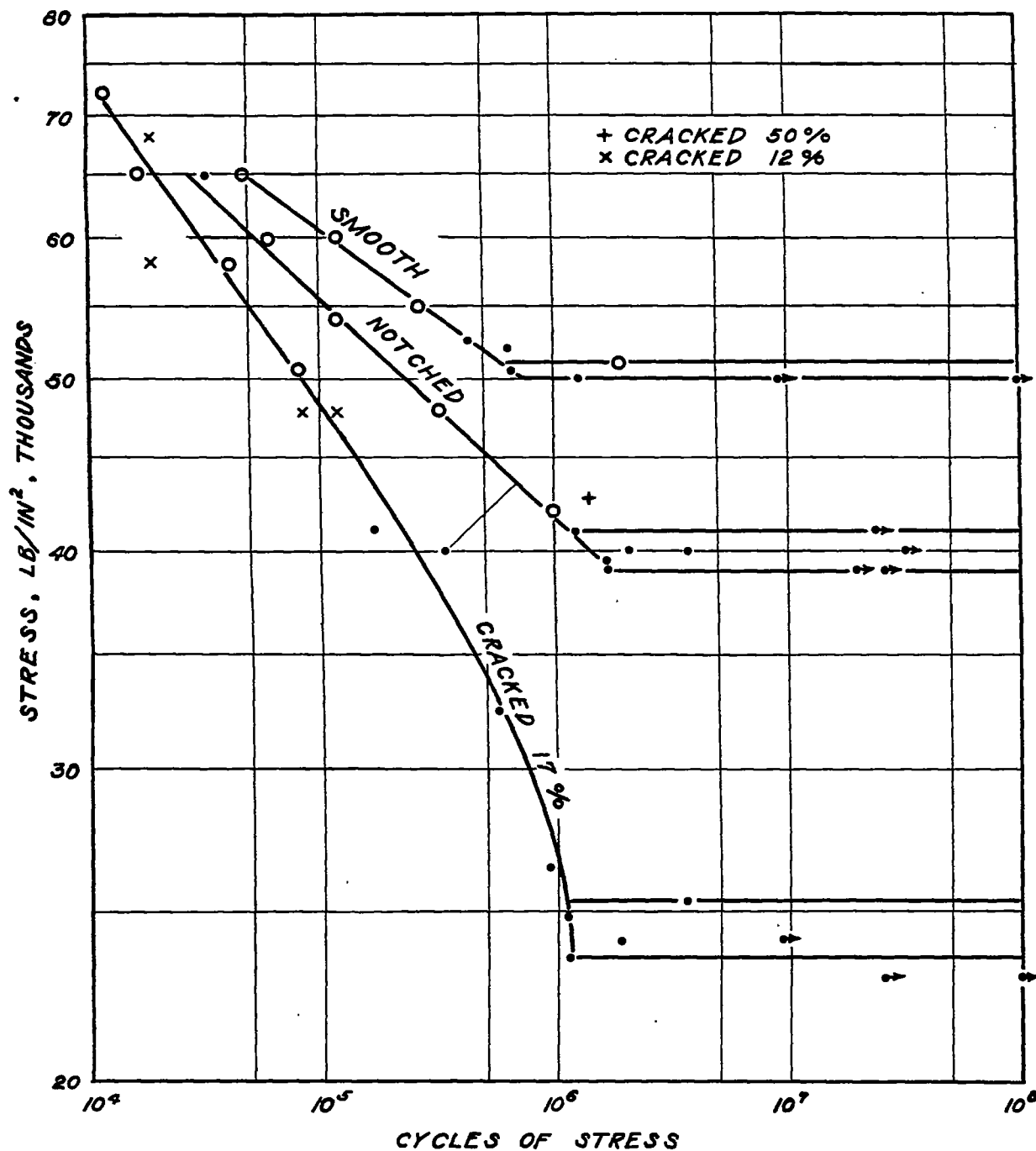


Figure 18.- S-N curves for SAE X4130 steel under three conditions of stress concentration. Large open points represent the median values from a group of specimens tested at the same stress. Small closed points are the results of individual tests.